

Joint Node Selection and Resource Allocation Optimization for Cooperative Sensing with a Shared Wireless Backhaul

Mingxin Chen, Ming-Min Zhao, An Liu, Min Li and Qingjiang Shi

arXiv:2405.16791v1 [cs.IT] 27 May 2024

Abstract—In this paper, we consider a cooperative sensing framework in the context of future multi-functional network with both communication and sensing ability, where one base station (BS) serves as a sensing transmitter and several nearby BSs serve as sensing receivers. Each receiver receives the sensing signal reflected by the target and communicates with the fusion center (FC) through a wireless multiple access channel (MAC) for cooperative target localization. To improve the localization performance, we present a hybrid information-signal domain cooperative sensing (HISDCS) design, where each sensing receiver transmits both the estimated time delay/effective reflecting coefficient and the received sensing signal sampled around the estimated time delay to the FC. Then, we propose to minimize the number of channel uses by utilizing an efficient Karhunen-Loève transformation (KLT) encoding scheme for signal quantization and proper node selection, under the Cramér-Rao lower bound (CRLB) constraint and the capacity limits of MAC. A novel matrix-inequality constrained successive convex approximation (MCSCA) algorithm is proposed to optimize the wireless backhaul resource allocation, together with a greedy strategy for node selection. Despite the high non-convexness of the considered problem, we prove that the proposed MCSCA algorithm is able to converge to the set of Karush-Kuhn-Tucker (KKT) solutions of a relaxed problem obtained by relaxing the discrete variables. Besides, a low-complexity quantization bit reallocation algorithm is designed, which does not perform explicit node selection, and is able to harvest most of the performance gain brought by HISDCS. Finally, numerical simulations are presented to show that the proposed HISDCS design is able to significantly outperform the baseline schemes.

Index Terms—Cooperative sensing, limited backhaul, multiple access channel, node selection

I. INTRODUCTION

Multi-functional network, which can provide both reliable communication and high-accuracy sensing services, is expected to play a crucial role in many application scenarios of the future 6G system such as autonomous driving, extended reality (XR) and multi-base radar sensing [2]–[5]. In these

scenarios, cooperative sensing by fusing perception data from multiple nodes is considered to be a powerful technique in various applications due to its inherent advantages [6]–[8]. On the one hand, cooperative sensing improves the accuracy of detection by combining information from multiple nodes, as the errors from one node can be mitigated by exploiting the sensing information from other nodes. On the other hand, cooperative sensing is envisioned to reduce the communication overhead significantly while ensure rapid adjustments to node deployment and localization strategy [8]. By sharing information between nodes, the overall cost of sensing networks can be reduced while maintaining or even improving the localization performance [9].

Generally, existing cooperative sensing schemes can be broadly categorized into two types, i.e., information-domain cooperative sensing (IDCS) and signal-domain cooperative sensing (SDCS). In IDCS, each sensing receiver extracts specific location information from the echo signals and then the fusion center (FC) fuses the extracted information for cooperative target localization [10], [11]. The common approaches of IDCS are usually based on the time-of-arrival (TOA) [12], [13], angle-of-arrival (AOA) [14], time-difference-of-arrival (TDOA) [15], received signal strength (RSS) [16], etc. Besides, the localization performance of IDCS is strongly relative to the employed data fusion algorithms [17], which can generally be categorized into two types, i.e., centralized algorithm and distributed algorithm. Centralized algorithms can offer more accurate position estimates in small networks with acceptable complexity [18], while distributed algorithms are also attractive since they can improve the network robustness and scalability [19]. However, the localization accuracy of IDCS is easily affected by non-line-of-sight (NLOS) propagation environments [20]. Besides, according to the law of data processing, extracting location information from echo signals always incurs certain information loss, which may lead to localization performance degradation.

In order to enhance the localization performance, the SDCS scheme has attracted great research interests recently [21]–[24], where each sensing receiver directly sends the echo signals to the FC for cooperative sensing. Specifically, in [21], the authors adopted a uniform quantizer for the echo signals in a cloud multiple-input multiple-output (MIMO) radar system, and Gaussian noise approximation for the quantization error was employed to evaluate the impact of finite backhaul capacity on target localization performance. The work [22] considered a multistatic radar setup, where distributed receive

M. Chen, M.M. Zhao, A. Liu and M. Li are with College of Information Science and Electronic Engineering, Zhejiang University, and also with Zhejiang Provincial Key Laboratory of Information Processing, Communication and Networking, Hangzhou 310027, China (Emails: {22331108, zmmblack, anliu, min.li}@zju.edu.cn). Q. Shi is with the School of Software Engineering, Tongji University, Shanghai 201804, China, and also with the Shenzhen Research Institute of Big Data, Shenzhen 518172, China (Email: shiqj@tongji.edu.cn).

Part of this paper is accepted for presentation at IEEE PIMRC 2024 [1], and the additional contributions of this journal version include the theoretical convergence proof of the MCSCA algorithm, detailed computational complexity analysis of the proposed algorithms, along with more comprehensive simulation results.

antennas were connected to the FC via limited backhaul links, and the localization performance was enhanced by jointly optimizing the code vector and the statistical properties of the noise introduced through backhaul quantization. In [23], a cooperative radar sensing system based on one-bit sampling of the received radar echoes was studied, and it was shown that the application of one-bit sampling significantly reduces the hardware cost, energy consumption and systematic complexity. Besides, the work [24], studied a low-bit direct localization method, where a Cramér-Rao lower bound (CRLB)-based objective function was designed to obtain the optimum quantization thresholds for each receiver, and it was shown that superior localization performance over the IDCS scheme can be achieved. As a brief summary, we can see that the SDCS scheme is able to achieve better sensing performance as compared to the IDCS scheme due to the ability of fully utilizing the information contained in the echoes. However, it comes with higher communication overhead and power consumption load, especially when the number of sensing receivers is large.

Motivated by the above, a hybrid information-signal domain cooperative sensing (HISDCS) framework is proposed in this paper in pursuit of an efficient tradeoff between IDCS and SDCS. In the proposed framework, carefully-quantized echo signals and some extracted location-related information from different receivers are fused in the FC via a limited-backhaul wireless multiple access channel (MAC). It is worth noting that by employing a subset of reliable nodes for localization, not only can the interference from unreliable nodes be reduced, but communication overhead can also be saved. Besides, we employ the CRLB as the sensing performance metric and formulate an optimization problem to minimize the number of channel uses by optimizing the backhaul resource (i.e., quantization bits) allocation and cooperative node selection, under MAC capacity constraints. The main contributions of this work are summarized as follows:

- 1) In the proposed HISDCS scheme, besides the estimated time delay and reflecting coefficient, we propose that each sensing receiver also transmits the echo signal sampled around the estimated delay with a proper quantization strategy to the FC. A Karhunen-Loève transformation (KLT) based encoding scheme is proposed for efficient echo signal quantization.
- 2) A novel matrix-inequality constrained successive convex approximation (MCSCA) algorithm is proposed for quantization bits allocation and a greedy strategy is designed for node selection. Besides, we theoretically prove the convergence of the MCSCA algorithm given a feasible initial solution. Additionally, a low-complexity quantization bit reallocation algorithm is proposed, which retains most of the performance gain offered by HISDCS.
- 3) Simulations results are presented to show the superiority of the proposed HISDCS scheme over some baseline designs, and it is shown that the proposed HISDCS scheme is able to achieve an efficient tradeoff between localization performance and communication cost.

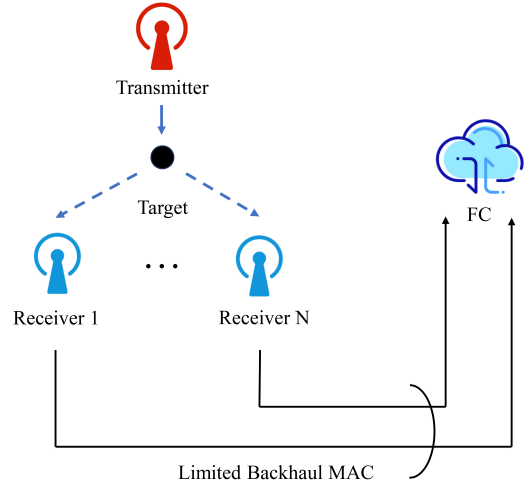


Fig. 1. Cooperative sensing system model

The rest of this paper is organized as follows. In Section II, we introduce the system model. Section III elaborates the HISDCS scheme. Section IV formulates an optimization problem and designs an efficient algorithm to solve the problem. Simulation results are provided in Section V and Section VI concludes the paper.

Notations: Scalars, vectors and matrices are respectively denoted by lower/upper case, boldface lower case and boldface upper case letters. $\Re(x)$ and $\Im(x)$ denote the real and imaginary parts of a complex number x , respectively. \mathbf{A}^T and \mathbf{A}^{-1} denote the transpose and inverse of matrix \mathbf{A} , respectively. \mathbf{I}_n denotes a $n \times n$ identity matrix. $\text{diag}(\mathbf{a})$ denotes a diagonal matrix with the elements in \mathbf{a} being its diagonal elements. $\|\mathbf{a}\|$ denotes the l_2 -norm of vector \mathbf{a} , and $\mathbf{A} \succeq \mathbf{B}$ means that $\mathbf{A} - \mathbf{B}$ is a positive semi-definite matrix.

II. SYSTEM MODEL

Consider a cooperative sensing system with $N + 1$ base stations (BSs), where one BS acts as the sensing transmitter while the other N BSs act as the sensing receivers, as shown in Fig. 1. The N sensing receivers are linked to the FC via a backhaul-limited Gaussian MAC. The sensing signal is sent by the transmitter, reflected by the target and then received by the N receivers. After certain signal processing and local location information extraction, the N receivers then quantify these local information and forward it to the FC. Finally, the FC estimates the target location based on the quantized information transmitted by the receivers.

Assuming that the transmitter and receivers are located at known positions (x^t, y^t) and (x_n^r, y_n^r) , $n \in [1, N]$, respectively, while the target is located at an unknown position, defined as $\boldsymbol{\theta} \triangleq [x, y]^T$. Besides, let $\sqrt{E}s(t)$ denote the lowpass equivalent of the signal transmitted from the transmitter, where E is the transmitted power and $s(t)$ is a power normalized waveform satisfying $\int_{T_c} |s(t)|^2 dt = 1$ with T_c being the signal duration time. Then, the echo signal received at the n -th receiver is

$$r_n(t) = \sqrt{E}\alpha_n s(t - \tau_n) + \omega_n(t), \quad (1)$$

where $\omega_n(t) \sim \mathcal{CN}(0, \sigma_n^2)$ is the complex Gaussian noise at the n -th receiver, $\alpha_n = \rho_n \xi_n$ is the effective reflecting coefficient of the n -th receiver, ρ_n is the corresponding path-loss coefficient and ξ_n is the reflection coefficient, which is assumed to be a complex random variable with unknown (deterministic) amplitude and random phase uniformly distributed between 0 and 2π . In addition, the time delay τ_n corresponding to the n -th receiver can be expressed as

$$\tau_n = \frac{\sqrt{(x^t - x)^2 + (y^t - y)^2} + \sqrt{(x_n^r - x)^2 + (y_n^r - y)^2}}{c}, \quad (2)$$

where c denotes the speed of light. After receiving the echo signals, the N sensing receivers first sample the signals as

$$r_n(kT_s) = \sqrt{E} \alpha_n s(kT_s - \tau_n) + \omega_n(kT_s), k \in [1, K], \quad (3)$$

where T_s is the sampling period. Then, the N sensing receivers quantize and process the sampled signals and communicate with the FC for cooperative sensing. Besides, it is worth noting that employing imprecise measurements from unreliable nodes may lead to localization accuracy deterioration [25]. Therefore, limiting the degree of cooperation and only using the measurements from the most informative nodes are essential for cooperative sensing.

Note that one baseline design for the considered problem is based on the IDCS scheme, where the n -th receiver first estimates the corresponding time delay τ_n and effective reflecting coefficient α_n from the received signal samples based on the ML rule and then transmits these estimated parameters to the FC. Finally, the FC estimates the target's location by using the received parameters from the N receivers by using the ML rule, again. Another baseline is based on the SDCS scheme, where each echo signal sample is uniformly quantized and then transmitted to the FC for localization [26].

The focus of this work is to combine the benefits of the IDCS and SDCS schemes by designing proper local processing and quantization schemes at each receiver and efficient cooperative node selection strategy to guarantee the estimation performance of θ at the FC while conserving the communication overhead.

III. HYBRID INFORMATION-SIGNAL DOMAIN COOPERATIVE SENSING

In order to enhance the sensing performance of the IDCS scheme while efficiently reduce the communication overhead of the SDCS scheme, a HISDCS scheme is proposed in this section by taking the limited MAC capacity into consideration. In the proposed design, each receiver first transmits the estimated time delay $\hat{\tau}_n$ and effective reflecting coefficient $\hat{\alpha}_n$ to the FC. Then, based on these estimated parameters, the FC solves a CRLB and MAC capacity constrained channel use number minimization problem to optimize the quantization bit allocation and node selection. Next, the FC sends the optimization results back to the N receivers through dedicated links. The selected receivers sample their received sensing signals around the estimated time delay and employ the KLT encoding scheme [27] to quantize these samples under the given quantization bit allocation. Finally, the quantized

samples are transmitted to the FC for sensing performance improvement. The main structure of the proposed scheme is provided in Fig. 2 and the key procedures mentioned above are detailed as follows.

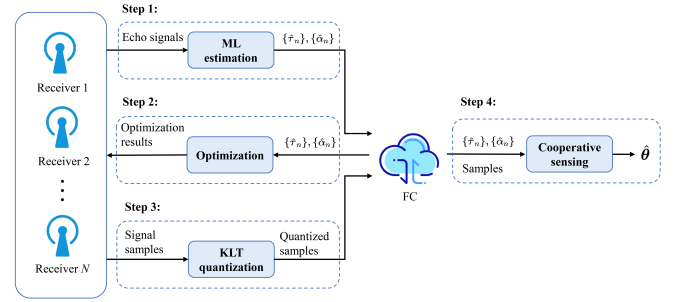


Fig. 2. Illustration of the proposed design

A. ML Estimation of Individual Delay and Effective Reflecting Coefficient

Define $\mathbf{r}_n = \{r_n(kT_s) | k = [1, K]\}$ as the vector containing all the echo signals received by the n -th receiver, then the probability density function (pdf) of \mathbf{r}_n against τ_n and α_n in the log domain is given as

$$\ln p(\mathbf{r}_n | \tau_n, \alpha_n) = -\frac{1}{\sigma_n^2} \sum_{k=1}^K \left| r_n(kT_s) - \sqrt{E} \alpha_n s(kT_s - \tau_n) \right|^2 + D_0, \quad (4)$$

where D_0 is a constant independent of τ_n and α_n . Thus, the ML estimator for τ_n and α_n can be expressed as

$$[\hat{\tau}_n, \hat{\alpha}_n] = \arg \max_{\tau_n, \alpha_n} \ln p(\mathbf{r}_n | \tau_n, \alpha_n). \quad (5)$$

Note that directly solving (5) generally requires a two-dimensional search, which incurs high computational complexity. Thus, we propose to first fix τ_n , then the optimal $\hat{\alpha}_n$ has a closed-form solution that can be expressed as:

$$\hat{\alpha}_n = \frac{\sum_{k=1}^K r_n(kT_s) s(kT_s - \tau_n)}{\sqrt{E} \sum_{k=1}^K [s(kT_s - \tau_n)]^2}, \quad (6)$$

Substituting (6) back into (5), the ML estimator for the time delay $\hat{\tau}_n$ can be obtained as

$$\hat{\tau}_n = \arg \max_{\tau_n} \left\{ -\frac{1}{\sigma_n^2} \sum_{k=1}^K \left| r_n(kT_s) - \sqrt{E} \hat{\alpha}_n s(kT_s - \tau_n) \right|^2 \right\}. \quad (7)$$

Since the CRLB offers a theoretical and achievable lower bound of any unbiased estimator, and similar to the model in [28], we assume that the estimated $\hat{\tau}_n$ is statistically related to the true parameter τ_n as follows:

$$\hat{\tau}_n = \tau_n + \omega_{\tau_n}, \quad (8)$$

where $\omega_{\tau_n} \sim \mathcal{N}(0, \text{CRLB}_{\hat{\tau}_n})$ is a Gaussian noise and its variance $\text{CRLB}_{\hat{\tau}_n}$ is the CRLB of τ_n at $\hat{\tau}_n$, given by [29]

$$\text{CRLB}_{\hat{\tau}_n} = \frac{1}{\frac{2E}{\sigma_n^2} |\hat{\alpha}_n|^2 \sum_{k=1}^K \left[\frac{\partial s(t)}{\partial t} \Big|_{t=kT_s - \hat{\tau}_n} \right]^2}. \quad (9)$$

B. Received Signal Quantization at Each Receiver

In this subsection, aiming to reduce the communication overhead (caused by sending all echo signal samples to the FC) and obtain high cooperation gain, we propose to send the received signals sampled around $\hat{\tau}_n$ to the FC. Suppose that each receiver has obtained the quantization bit allocation scheme from the FC (the details are provided in Section IV), the KLT based encoding scheme is thus employed to quantize these samples, which is shown to maximize the coding gain for Gaussian sources [30].

First, we introduce a sample index set at the n -th receiver, denoted by $\mathcal{K}_n = \{k_n \in \mathcal{Z} \mid \hat{\tau}_n - \frac{T_d}{2} \leq k_n T_s \leq \hat{\tau}_n + \frac{T_d}{2}\}$, where T_d is the sampling interval length and the size of \mathcal{K}_n is K_n . Then, we can obtain a $2K_n \times 1$ vector which collects the real and imaginary parts of the signal samples at the n -th receiver, i.e.,

$$\mathbf{r}_n = [\{\Re(r_n(k_n T_s)), k_n \in \mathcal{K}_n\}, \{\Im(r_n(k_n T_s)), k_n \in \mathcal{K}_n\}]^T. \quad (10)$$

Second, in order to efficiently quantize the sampled signals, it is crucial to utilize the statistical information contained in \mathbf{r}_n . However, it is very difficult to directly analyze the exact distribution of \mathbf{r}_n . To make the analysis tractable, we approximate $r_n(k_n T_s)$ by considering its first-order Taylor expansion at $\hat{\tau}_n$, which can be expressed as

$$r_n(k_n T_s) \approx \sqrt{E} \alpha_n \left[\omega_{\tau_n} \frac{\partial s(t)}{\partial t} \Big|_{t=k_n T_s - \hat{\tau}_n} + s(k_n T_s - \hat{\tau}_n) \right] + \omega_n(k_n T_s). \quad (11)$$

Note that both $\omega_n(k_n T_s)$ and ω_{τ_n} are Gaussian distributed, we can prove that the approximate value of \mathbf{r}_n in (11) also obeys Gaussian distribution with its covariance matrix $\mathbf{Q}_{\mathbf{r}_n}$ given by

$$\mathbf{Q}_{\mathbf{r}_n} = E \cdot \text{CRLB}_{\hat{\tau}_n} \mathbf{q}_{\mathbf{r}_n} \mathbf{q}_{\mathbf{r}_n}^T + \frac{1}{2} \sigma_n^2 \mathbf{I}_{2K_n}, \quad (12)$$

where $\mathbf{q}_{\mathbf{r}_n} = [\{\Re(\hat{\alpha}_n) \frac{\partial s(t)}{\partial t} \Big|_{t=k_n T_s - \hat{\tau}_n}, k_n \in \mathcal{K}_n\}, \{\Im(\hat{\alpha}_n) \frac{\partial s(t)}{\partial t} \Big|_{t=k_n T_s - \hat{\tau}_n}, k_n \in \mathcal{K}_n\}]^T$. The proof is straightforward and is omitted for conciseness.

Finally, based on the above approximation and statistical knowledge of \mathbf{r}_n , we can apply the KLT based encoding scheme to quantize \mathbf{r}_n via the following two steps.

In the first step, we obtain $\mathbf{Q}_{\mathbf{r}_n} = \mathbf{U} \mathbf{\Lambda} \mathbf{U}^T$ via eigenvalue decomposition, where the diagonal matrix $\mathbf{\Lambda} = \text{diag}(\gamma_{n1}, \gamma_{n2}, \dots, \gamma_{n(2K_n)})$ collects all the eigenvalues of $\mathbf{Q}_{\mathbf{r}_n}$ and that satisfy $\gamma_{n1} = 2\gamma_{n2} = \dots = 2\gamma_{n(2K_n)} = \sigma_n^2$. Then, by transforming \mathbf{r}_n using KLT, we can obtain the following transformed vector:

$$\mathbf{r}_{nC} = \mathbf{U}^T \mathbf{r}_n. \quad (13)$$

Since the covariance matrix of the transformed vector \mathbf{r}_{nC} is the diagonal matrix $\mathbf{\Lambda}$, all the elements in \mathbf{r}_{nC} are independent of each other and satisfy

$$[\mathbf{r}_{nC}]_j \sim \mathcal{N} \left([\mathbf{U}^T \bar{\mathbf{r}}_n]_j, \gamma_{nj} \right), j \in [1, 2K_n]. \quad (14)$$

In the second step, a Lloyd quantizer [31] is applied to quantize $[\mathbf{r}_{nC}]_j, j \in [1, 2K_n]$. Since the locations of the N

receivers are different and the impacts of their received signals on sensing performance are distinct, $[\mathbf{r}_{nC}]_j, j \in [1, 2K_n]$ can be quantized using different numbers of quantization bits. Nevertheless, the total number of available quantization bits is constrained by the MAC channel capacity.

C. Target Localization at the FC

Suppose that the FC can obtain the estimated time delays $\{\hat{\tau}_n\}$ and effective reflecting coefficients $\{\hat{\alpha}_n\}$ (information-domain) at the receivers with negligible quantization error, then the eigenmatrix \mathbf{U} can be acquired with negligible quantization loss, which implicitly contains the information-domain signals $\{\hat{\tau}_n, \hat{\alpha}_n\}$. After receiving the quantized signal samples $\tilde{\mathbf{r}}_{nC}$ (signal-domain) from the N receivers, the FC is able to recover the target location by fusing these signal-domain and information-domain measurements, i.e., $\{\hat{\tau}_n, \hat{\alpha}_n\}$ and $\{[\mathbf{r}_{nC}]_j, j \in [1, 2K_n]\}$.

Specifically, to evaluate the impact of signal quantization on the sensing performance, we introduce the Gaussian quantization error model [32], based on which the j -th quantized signal at the n -th receiver, i.e., $[\tilde{\mathbf{r}}_{nC}]_j$, can be expressed as

$$[\tilde{\mathbf{r}}_{nC}]_j = [\mathbf{r}_{nC}]_j + q_{nj}, \quad (15)$$

where $q_{nj} \sim \mathcal{N}(0, \eta_{nj})$ is the additive Gaussian quantization error and $\eta_{nj} = \frac{\gamma_{nj}}{2^{2X_{nj}-1}}$ is the lower bound of the variance of q_{nj} , which can be obtained by

$$I([\tilde{\mathbf{r}}_{nC}]_j; [\mathbf{r}_{nC}]_j) = \frac{1}{2} \log_2 \left(\frac{\eta_{nj} + \gamma_{nj}}{\eta_{nj}} \right) \leq X_{nj}, \quad (16)$$

with X_{nj} denoting the number of bits allocated for quantizing $[\mathbf{r}_{nC}]_j$ and $I([\tilde{\mathbf{r}}_{nC}]_j; [\mathbf{r}_{nC}]_j)$ denoting the mutual information between $[\tilde{\mathbf{r}}_{nC}]_j$ and $[\mathbf{r}_{nC}]_j$. According to the rate-distortion theorem [31], the above quantization variance can be achieved by using the KLT based encoding scheme if (16) holds.

Then, by performing inverse linear transformation on $\tilde{\mathbf{r}}_{nC}$, i.e., multiplying $\tilde{\mathbf{r}}_{nC}$ on the left by eigenmatrix \mathbf{U} , we are able to recover the received signal samples by

$$\tilde{\mathbf{r}}_n = \mathbf{U} \tilde{\mathbf{r}}_{nC} = \mathbf{r}_n + \mathbf{U} \mathbf{q}_n, \quad (17)$$

where $\mathbf{U} \mathbf{q}_n \sim \mathcal{N}(\mathbf{0}, \mathbf{Q}_n)$ is the quantization error vector of \mathbf{r}_n and \mathbf{Q}_n is given by

$$\mathbf{Q}_n = \mathbf{U} \text{diag}([\eta_{n1}, \dots, \eta_{n(2K_n)}]) \mathbf{U}^T. \quad (18)$$

Finally, the FC estimates the target location by resorting to the ML rule. Let $\Omega \subseteq \{1, 2, \dots, N\}$ denote the selected receivers (the detailed selection strategy will be introduced in Section IV), then the received signal samples available at the FC can be represented as $\tilde{\mathbf{r}}_\Omega = \{\tilde{\mathbf{r}}_n \mid n \in \Omega\}$. Therefore, the ML estimation of $\boldsymbol{\theta} = [x, y]^T$ can be obtained by

$$\hat{\boldsymbol{\theta}} = \arg \max_{\boldsymbol{\theta}} \ln p(\tilde{\mathbf{r}}_\Omega \mid \boldsymbol{\theta}), \quad (19)$$

where

$$\begin{aligned} \ln p(\tilde{\mathbf{r}}_\Omega \mid \boldsymbol{\theta}) = & -\frac{1}{2} \sum_{n \in \Omega} \left[(\tilde{\mathbf{r}}_n - \mathbf{s}_n)^T (\mathbf{Q}_{\omega_n} + \mathbf{Q}_n)^{-1} (\tilde{\mathbf{r}}_n - \mathbf{s}_n) \right] + D_2, \end{aligned} \quad (20)$$

and D_2 is a constant uncorrelated with θ , $\mathbf{Q}_{\omega_n} = \frac{1}{2}\sigma_n^2\mathbf{I}_{2K_n}$ is a diagonal matrix and $\mathbf{s}_n = [\{\sqrt{E}\Re(\hat{\alpha}_n)s(k_nT_s - \tau_n), k_n \in \mathcal{K}_n\}, \{\sqrt{E}\Im(\hat{\alpha}_n)s(k_nT_s - \tau_n), k_n \in \mathcal{K}_n\}]^T$.

IV. PROBLEM FORMULATION AND ALGORITHM DESIGN

In this section, we formulate an optimization problem to minimize the communication cost (i.e., the number of channel uses), under the CRLB constraint that ensures the sensing performance and the MAC capacity constraints between the sensing receivers and the FC. The number of quantization bits at each receiver and the set of selected receivers are jointly optimized by proposing a novel MCSCA algorithm and a greedy node selection strategy. Besides, we prove that the proposed MCSCA algorithm is guaranteed to converge to the set of Karush-Kuhn-Tucker (KKT) solutions, and a simple greedy bit reallocation algorithm is further designed for lower computational complexity.

A. Optimization Problem Formulation

In this work, we employ the well-known CRLB as the sensing performance metric, since it offers a theoretical lower bound on the best achievable estimation accuracy under given observations [30]. Specifically, the CRLB of θ at $\hat{\theta}$ can be obtained as

$$\text{CRLB}_{\hat{\theta}} = \text{tr}[\mathbf{J}^{-1}(\hat{\theta})], \quad (21)$$

where $\mathbf{J}(\theta)$ denotes the Fisher information matrix (FIM), which is given by

$$\begin{aligned} \mathbf{J}(\theta) &= E_{\tilde{\mathbf{r}}_{\Omega}|\theta} \left\{ -\frac{\partial^2}{\partial\theta\partial\theta^T} \ln p(\tilde{\mathbf{r}}_{\Omega} | \theta) \right\} \\ &= \sum_{n \in \Omega} \frac{\partial \mathbf{s}_n}{\partial \theta} (\mathbf{Q}_{\omega_n} + \mathbf{Q}_n)^{-1} \left(\frac{\partial \mathbf{s}_n}{\partial \theta} \right)^T. \end{aligned} \quad (22)$$

Then, according to the MAC channel capacity limits [33], the number of quantization bits $\{X_{nj}\}$ must satisfy the following conditions for each possible non-empty subset \mathcal{S} of Ω :

$$\sum_{n \in \mathcal{S}} \frac{\sum_{j=1}^{2K_n} X_{nj}}{W} \leq \log \left(1 + \frac{\sum_{n \in \mathcal{S}} P_n g_n}{N_0} \right), \quad (23)$$

for all $\mathcal{S} \subseteq \Omega$,

where W is the number of channel uses, N_0 denotes the noise power, P_n and g_n represent the transmit power at the n -th sensing receiver and the channel gain between the n -th receiver and the FC, respectively. Therefore, the considered optimization problem can be formulated as¹

$$\min_{\Omega, X_{nj}, W} W \quad (24a)$$

s.t. (23),

$$\text{CRLB}_{\hat{\theta}} \leq \epsilon, \quad (24b)$$

$$W \in \mathcal{N}^+, \quad (24c)$$

$$X_{nj} \in \mathcal{N}, j \in [1, 2K_n], n \in \Omega, \quad (24d)$$

¹Note that in this work, we assume that the N receivers transmit signals using the same power, thus the transmit power P_n is not an optimization variable.

where W is minimized as the objective function to reduce the communication cost and constraint (24b) is introduced to guarantee certain sensing performance. It is noteworthy that the feasibility of problem (24) can be ensured by setting a proper value of ϵ that exceeds the minimum achievable CRLB (denoted by ϵ^*), which can be easily obtained by letting $X_{nj} \rightarrow \infty$ and then calculating the corresponding CRLB through (21).

Problem (24) is challenging to solve because 1) the optimization variables are discrete and intricately coupled in the constraints; 2) the CRLB constraint (24b) is highly non-convex which involves matrix inversion operation; and 3) selecting appropriate cooperative nodes is a combinatorial problem which is in general NP-hard. Generally, there is no efficient method for solving the non-convex problem (24) optimally.

B. Algorithm Design

To address the above challenges, we propose in this work to decouple the optimization of the quantization bit numbers at each receiver $\{X_{nj}\}$, the required channel use number W , and the selected node set Ω . Specifically, we first present an efficient MCSCA algorithm to optimize $\{X_{nj}\}$ and W with given Ω , and then a greedy node selection strategy is presented to optimize Ω based on the MCSCA algorithm, which is able to find a high-quality solution of problem (24) effectively.

1) MCSCA Algorithm for Quantization Bit Allocation:

With given node selection, problem (24) is still difficult to solve due to the discrete variables $\{X_{nj}\}$ and W , and non-convex CRLB constraint. To tackle these challenges, we first slack the discrete variables $\{X_{nj}\}$ and W into continuous ones. Then, in order to resolve the difficulty caused by the matrix inversion operation in CRLB, we introduce a 2×2 auxiliary matrix \mathbf{M} which satisfies

$$\mathbf{M} \succeq \mathbf{J}^{-1}(\hat{\theta}). \quad (25)$$

Since $\mathbf{J}^{-1}(\hat{\theta}) \succeq \mathbf{0}$, (25) can be equivalently transformed into the following positive semidefinite constraint:

$$\mathbf{G} = \begin{bmatrix} \mathbf{M} & \mathbf{I}_2 \\ \mathbf{I}_2 & \mathbf{J}(\hat{\theta}) \end{bmatrix} \succeq \mathbf{0}, \quad (26)$$

where \mathbf{I}_2 is a 2×2 identity matrix. Thus, according to above transformations, the quantization bit allocation sub-problem under given Ω can be obtained by

$$\min_{\{X_{nj}\}, W, \mathbf{M}} W \quad (27a)$$

s.t. (23), (26)

$$\text{tr}(\mathbf{M}) \leq \epsilon, \quad (27b)$$

$$\{W, X_{nj}\} \in \mathcal{R}^+, j \in [1, 2K_n], n \in \Omega. \quad (27c)$$

Next, since the eigenmatrix \mathbf{U} is an orthogonal matrix, $\mathbf{J}(\hat{\theta})$ can be equivalently rewritten as

$$\begin{aligned} \mathbf{J}(\hat{\theta}) &= \\ &= \sum_{n \in \Omega} \frac{\partial \mathbf{s}_n}{\partial \theta} \mathbf{U} \text{diag}([y_n(X_{n1}), \dots, y_n(X_{n(2K_n)})]) \left(\frac{\partial \mathbf{s}_n}{\partial \theta} \mathbf{U} \right)^T, \end{aligned} \quad (28)$$

where $y_n(X_{nj})$ is given by

$$y_n(X_{nj}) = \frac{2^{2X_{nj}-1}}{\gamma_{nj} + 2^{2X_{nj}-2}\sigma_n^2}, n \in \Omega, j \in [1, 2K_n]. \quad (29)$$

As can be seen, since $y_n(X_{nj})$ in (29) is a non-convex function with respect to X_{nj} , constraint (26) is a non-convex constraint and difficult to handle. Besides, since (26) is a matrix-inequality constraint, the existing successive convex approximation (SCA) algorithm [34] cannot be directly applied. Therefore, we propose the MCSCA algorithm to tackle the problem (27) effectively, where $\{X_{nj}\}$ are iteratively updated by solving a sequence of convex optimization problems.

Specifically, at the t -th iteration, a surrogate function $u_n^t(X_{nj})$ is constructed for each $y_n(X_{nj})$, which can be viewed as the tangent function of $y_n(X_{nj})$ at point X_{nj}^t and is given by

$$u_n^t(X_{nj}) = (X_{nj} - X_{nj}^t)\nabla y_n(X_{nj}^t) + y_n(X_{nj}^t), \quad (30)$$

where

$$\begin{aligned} \nabla y_n(X_{nj}^t) &= \frac{\ln 2 \cdot 2^{2X_{nj}^t} \gamma_{nj}}{(\gamma_{nj} + 2^{2X_{nj}^t-2})^2 \sigma_n^2}, \\ y_n(X_{nj}^t) &= \frac{2^{2X_{nj}^t-1}}{\gamma_{nj} + 2^{2X_{nj}^t-2}\sigma_n^2}. \end{aligned} \quad (31)$$

Then, we can obtain a surrogate FIM $\bar{\mathbf{J}}^t(\hat{\boldsymbol{\theta}})$ by substituting (30) into (28) and a surrogate matrix $\bar{\mathbf{G}}^t$ by replacing $\bar{\mathbf{J}}(\hat{\boldsymbol{\theta}})$ in (26) with $\bar{\mathbf{J}}^t(\hat{\boldsymbol{\theta}})$. Therefore, by employing a small positive number $\mu > 0$, we have the following strongly convex problem:

$$\min_{\mathbf{x}, \{X_{nj}\}, W, \mathbf{M}} W + \mu \|\mathbf{x} - \mathbf{x}^t\|^2 \quad (32a)$$

s.t. (27c),

$$\text{tr}(\mathbf{M}) + \mu \|\mathbf{x} - \mathbf{x}^t\|^2 \leq \epsilon, \quad (32b)$$

$$\bar{\mathbf{G}}^t = \begin{bmatrix} \mathbf{M} & \mathbf{I}_2 \\ \mathbf{I}_2 & \bar{\mathbf{J}}^t(\hat{\boldsymbol{\theta}}) \end{bmatrix} \succeq \mu \|\mathbf{x} - \mathbf{x}^t\|^2 \mathbf{I}_4, \quad (32c)$$

$$\sum_{n \in \mathcal{S}} \frac{\sum_{j=1}^{2K_n} X_{nj}}{W} + \mu \|\mathbf{x} - \mathbf{x}^t\|^2 \leq \quad (32d)$$

$$\log \left(1 + \frac{\sum_{n \in \mathcal{S}} P_n g_n}{N_0} \right), \text{ for all } \mathcal{S} \subseteq \Omega,$$

$$\| [X_{nj} - X_{nj}^t] \|^2 \leq (\beta^t)^2, \quad (32e)$$

where $\mathbf{x} \triangleq [\{X_{nj}\}, W, \text{vec}(\mathbf{M})^T]^T$ and the term $\mu \|\mathbf{x} - \mathbf{x}^t\|^2$ is added to ensure the strong convexity of the surrogate functions. Besides, $\{\beta^t\}$ in (32e) is a decreasing sequence satisfying $\beta^t \rightarrow 0$ and $\sum_t \beta^t = \infty$, which is introduced to gradually decrease the variable updating speed and ensure that the algorithm finally converges. Based on the above approximation, \mathbf{x}^{t+1} , $\{X_{nj}^{t+1}\}$ and W^{t+1} are obtained by solving (32) via existing software solvers, such as CVX [35].

The main steps of the proposed MCSCA algorithm are summarized in Algorithm 1, and it can be proved that Algorithm 1 is guaranteed to converge to the set of KKT solutions of problem (27). The details will be presented in the following.

Algorithm 1 Proposed MCSCA Algorithm for Quantization Bits Allocation

Input: Ω , $\{\hat{r}_n\}$, $\{\hat{\alpha}_n\}$, $\{\sigma_n^2\}$, $\{P_n\}$, $\{g_n\}$, N_0 and $\{\beta^t\}$.

Output: $\{X_{nj}^0\}$ and \bar{W} .

- 1: **Initialize** $\{X_{nj}^0\}$, $t = 0$.
 - 2: **repeat**
 - 3: Update the surrogate functions $u_n^t(X_{nj})$ according to (29);
 - 4: Solve problem (32) to obtain $\{X_{nj}^{t+1}\}$ and W^{t+1} ;
 - 5: $t = t + 1$;
 - 6: **until** some convergence criterion is met
-

Remark 1. It is noteworthy that to make the overall problem tractable, we have ignored the discrete constraints and relaxed $\{X_{nj}\}$ as continuous variables in problem (27). After obtaining the optimized quantization bit allocation, we can simply round up the continuous bit numbers to obtain a discrete solution, i.e.,

$$X_{nj}^* = \lceil \bar{X}_{nj} \rceil, n \in \Omega, j \in [1, 2K_n]. \quad (33)$$

and the final channel use number W^* is set to be the minimum integer that satisfies the constraint (23).

2) *Convergence Analysis for the MCSCA Algorithm:* In order to facilitate our convergence analysis of the MCSCA algorithm, we propose to properly modify the problem formulation and algorithm design, which are detailed as follows.

First, the positive semidefinite constraint (26) is equivalent to the following constraint:

$$\lambda_{\min}(\mathbf{G}) \geq 0, \quad (34)$$

where $\lambda_{\min}(\mathbf{G})$ denotes the minimum eigenvalue of \mathbf{G} . Since the smallest eigenvalue of a symmetric matrix is equal to its minimum Rayleigh quotient, for $\forall \gamma \in [0, 1]$, we have

$$\begin{aligned} &\lambda_{\min}(\gamma \mathbf{G} + (1 - \gamma) \mathbf{G}') \\ &= \min_{\mathbf{v}} \frac{\mathbf{v}^T (\gamma \mathbf{G} + (1 - \gamma) \mathbf{G}') \mathbf{v}}{\mathbf{v}^T \mathbf{v}} \\ &= \min_{\mathbf{v}} \left\{ \gamma \frac{\mathbf{v}^T \mathbf{G} \mathbf{v}}{\mathbf{v}^T \mathbf{v}} + (1 - \gamma) \frac{\mathbf{v}^T \mathbf{G}' \mathbf{v}}{\mathbf{v}^T \mathbf{v}} \right\} \\ &\geq \gamma \min_{\mathbf{v}_1} \frac{\mathbf{v}_1^T \mathbf{G} \mathbf{v}_1}{\mathbf{v}_1^T \mathbf{v}_1} + (1 - \gamma) \min_{\mathbf{v}_2} \frac{\mathbf{v}_2^T \mathbf{G}' \mathbf{v}_2}{\mathbf{v}_2^T \mathbf{v}_2} \\ &= \gamma \lambda_{\min}(\mathbf{G}) + (1 - \gamma) \lambda_{\min}(\mathbf{G}'). \end{aligned} \quad (35)$$

Hence, $\lambda_{\min}(\mathbf{G})$ is a concave function of \mathbf{G} , and problem (27) can be equivalently reformulated as follows:

$$\min_{\mathbf{x} \in \mathcal{X}} f_0(\mathbf{x}) \quad (36a)$$

$$\text{s.t. } f_i(\mathbf{x}) \leq 0, i = 1, \dots, m, \quad (36b)$$

where \mathcal{X} is the domain of $\mathbf{x} \triangleq [\{X_{nj}\}, W, \text{vec}(\mathbf{M})^T]^T$, $f_0(\mathbf{x}) \triangleq W$ and $f_i(\mathbf{x}) \triangleq -\lambda_{\min}(\mathbf{G})$. The rest constraints in (36b), i.e., $f_i(\mathbf{x}) \leq 0, i \in [2, m]$, can be easily obtained from (23) and (27b), the details are omitted here for brevity.

Next, according to the structure of the MCSCA algorithm, in each iteration t , we replace the objective function and

constraints $f_i(\mathbf{x}), i \in [0, m]$ by the following strongly convex surrogate functions $\bar{f}_i^t(\mathbf{x}), i \in \{0, \dots, m\}$:

$$\bar{f}_i^t(\mathbf{x}) = \begin{cases} -\lambda_{\min}(\bar{\mathbf{G}}^t) + \mu \|\mathbf{x} - \mathbf{x}^t\|^2, & i = 1, \\ f_i(\mathbf{x}) + \mu \|\mathbf{x} - \mathbf{x}^t\|^2, & i \in \{0\} \cup \{2, \dots, m\}, \end{cases} \quad (37)$$

where $\mu > 0$ is a small positive number. Note that in (37) the convexity of $-\lambda_{\min}(\bar{\mathbf{G}}^t)$ and $f_i(\mathbf{x}), i \in \{0\} \cup [2, m]$ can be easily established, and the term $\mu \|\mathbf{x} - \mathbf{x}^t\|^2$ is added to ensure the strong convexity of $\bar{f}_i^t(\mathbf{x}), i \in [0, m]$.

Accordingly we solve the following surrogate convex problem the t -th iteration :

$$\mathbf{x}^{t+1} = \arg \min_{\mathbf{x} \in \mathcal{X}} \bar{f}_0^t(\mathbf{x}) \quad (38a)$$

$$\text{s.t. } \bar{f}_i^t(\mathbf{x}) \leq 0, i = 1, \dots, m, \quad (38b)$$

$$\|\mathbf{x} - \mathbf{x}^t\|^2 \leq (\beta^t)^2. \quad (38c)$$

Note that although only the elements $\{X_{nj}\}$ in \mathbf{x} are required to satisfy the constraint (38c), we impose this constraint on all the optimization variables in \mathbf{x} , which will simplify the convergence proof, but will not affect the performance of the proposed MCSCA algorithm (as validated via numerical simulations).

Then, we introduce some lemmas which are crucial for our proof.

Lemma 1. Consider the following optimization problem which is obtained by removing the constraint (38c) from problem (38):

$$\bar{\mathbf{x}}^t = \arg \min_{\mathbf{x} \in \mathcal{X}} \bar{f}_0^t(\mathbf{x}) \quad (39a)$$

$$\text{s.t. } \bar{f}_i^t(\mathbf{x}) \leq 0, i = 1, \dots, m. \quad (39b)$$

Let $\{\mathbf{x}^t\}_{t=1}^{\infty}$ and $\{\bar{\mathbf{x}}^t\}_{t=1}^{\infty}$ denote the sequences of iterates generated by the proposed MCSCA algorithm when solving problems (38) and (39), respectively, then we have

$$\lim_{t \rightarrow \infty} \|\bar{\mathbf{x}}^t - \mathbf{x}^t\| = 0. \quad (40)$$

Proof. Please refer to Appendix A for the proof. \square

Lemma 2. [36] Consider a subsequence $\{\mathbf{x}^{t_j}\}_{j=1}^{\infty}$ converging to a limit point \mathbf{x}^* . There exist continuous functions $\hat{f}_i(\mathbf{x}), i = 1, \dots, m$ that satisfy

$$\lim_{j \rightarrow \infty} \bar{f}_i^{t_j}(\mathbf{x}) = \hat{f}_i(\mathbf{x}), \forall \mathbf{x} \in \mathcal{X}, \quad (41)$$

with the Slater's condition satisfied at \mathbf{x}^* if there exist $\mathbf{x} \in \text{relint}\mathcal{X}$ such that

$$\hat{f}_i(\mathbf{x}) < 0, \forall i = 1, \dots, m. \quad (42)$$

Based on Lemmas 1 and 2, we are ready to prove the following convergence result.

Theorem 1. Let \mathbf{x}^0 denote an initial feasible point, the limiting point \mathbf{x}^* of $\{\mathbf{x}^t\}_{t=1}^{\infty}$ which satisfies the Slater's condition is a stationary solution of problem (34).

Proof. According to Lemma 1, the constraint (38c) is inactive when $t \rightarrow \infty$, which implies that problem (38) is equivalent

to problem (39) when t is sufficiently large. Therefore, based on (40) and (41), we have

$$\mathbf{x}^* = \arg \min_{\mathbf{x} \in \mathcal{X}} \hat{f}_0(\mathbf{x}) \quad (43a)$$

$$\text{s.t. } \hat{f}_i(\mathbf{x}) \leq 0, i = 1, \dots, m, \quad (43b)$$

as $t \rightarrow \infty$ and since the Slater's condition is satisfied, the KKT conditions of problem (43) indicates that there exist Lagrange dual variables $\lambda_1, \dots, \lambda_m$ such that

$$\begin{aligned} \nabla \hat{f}_0(\mathbf{x}^*) + \sum_i \lambda_i \nabla \hat{f}_i(\mathbf{x}^*) &= \mathbf{0}, \\ \hat{f}_i(\mathbf{x}^*) &\leq 0, \forall i = 1, \dots, m, \\ \lambda_i \hat{f}_i(\mathbf{x}^*) &= 0, \forall i = 1, \dots, m. \end{aligned} \quad (44)$$

Then, owing to the fact that the surrogate function $u^t(X_{nj})$ is the tangent function of $y^t(X_{nj})$ according to (29), and using (41), we have the following facts:

$$\begin{aligned} \|\nabla \hat{f}_i(\mathbf{x}^*) - \nabla f_i(\mathbf{x}^*)\| &= 0, \forall i = 1, \dots, m, \\ |\hat{f}_i(\mathbf{x}^*) - f_i(\mathbf{x}^*)| &= 0, \forall i = 1, \dots, m. \end{aligned} \quad (45)$$

Finally, it follows from (44) and (45) that \mathbf{x}^* also satisfies the KKT conditions of the original problem (36). Hence, \mathbf{x}^* is a stationary point of problem (36). This completes the proof. \square

3) Node Selection Strategy: For node selection, we propose in this work a greedy strategy to iteratively exclude the most non-informative node from cooperation, such that the communication cost can be further reduced.

Specifically, we first initialize the selected node set as $\Omega^0 = \{1, 2, \dots, N\}$ by taking all the nodes into consideration. In each iteration t_1 , Algorithm 1 is executed to obtain the optimized quantization bit numbers $\{\bar{X}_{nj}^{t_1}\}$ and channel use number \bar{W}^{t_1} according to the current set of selected nodes Ω^{t_1} . Then, in the next iteration $t_1 + 1$, the node with the minimum number of allocated quantization bits, denoted by n^{t_1} , is excluded from Ω^{t_1} because generally this node exhibits the least contribution to localization performance improvement. Consequently, a new selected node set is obtained by $\Omega^{t_1+1} = \Omega^{t_1} \setminus n^{t_1}$. Next, Algorithm 1 is executed again to obtain the new optimized quantization bit numbers $\{\bar{X}_{nj}^{t_1+1}\}$ and channel use number \bar{W}^{t_1+1} . If $\bar{W}^{t_1+1} > \bar{W}^{t_1}$, i.e., excluding the current node n^{t_1} does not lead to a reduction in the number of channel uses, then the algorithm is terminated; otherwise, the above greedy node selection process continues. It is worth noting that in the above iterative process, Algorithm 1 may not be feasible, this indicates that the current node selection scheme cannot satisfy the CRLB constraint. In this case, the proposed algorithm should also be terminated. The above strategy is summarized in Algorithm 2.

Algorithm 2 Proposed Greedy Node Selection Strategy**Input:** $\{\hat{\tau}_n\}$, $\{\hat{\alpha}_n\}$, $\{\sigma_n^2\}$, $\{B_n\}$, $\{P_n\}$, $\{g_n\}$ and N_0 .**Output:** $\{X_{nj}^*\}$, W^* and Ω^* .

- 1: **Initialize** $\Omega^0 = \{1, 2, \dots, N\}$, $t_1 = 0$, $W^{-1} = +\infty$.
- 2: **repeat**
- 3: Execute Algorithm 1 to obtain $\{\bar{X}_{nj}^{t_1}\}$, \bar{W}^{t_1} and n^{t_1} according to Ω^{t_1} ;
- 4: Update the set of selected nodes by $\Omega^{t_1+1} = \Omega^{t_1} \setminus n^{t_1}$;
- 5: $t_1 = t_1 + 1$;
- 6: **until** $(\bar{W}^{t_1} > \bar{W}^{t_1-1})$ or the Algorithm 1 is infeasible
- 7: $\Omega^* = \Omega^{t_1-1}$, $X_{nj}^* = \bar{X}_{nj}^{t_1-1}$ and $W^* = \bar{W}^{t_1-1}$;

Next, we endeavor to analyze the computational complexity of the proposed greedy node selection algorithm. It is imperative to note that within each iteration of Algorithm 2, the proposed MCSCA algorithm is executed once. Hence, the complexity of Algorithm 2 is dominated by the complexity of the MCSCA algorithm. Besides, in each iteration of the MCSCA algorithm, problem (32) is solved by resorting to the interior-point method (IPM), whose complexity can be expressed as [37]

$$C_{IPM} = n\sqrt{4 + 2^N}[(4^3 + 2^N) + n(4^2 + 2^N) + n^2], \quad (46)$$

where $n = 2K_n N + 5$. Let L denote the average iteration number of the MCSCA algorithm, then the complexity order of the MCSCA algorithm can be obtained as

$$C_1 = O(2^{3N/2} N^2 K_n^2 L). \quad (47)$$

Next, note that in the worst-case scenario, our greedy strategy executes the MCSCA algorithm N times, the overall worst-case complexity order of Algorithm 2 is given by

$$C_2 = O\left(\sum_{i=1}^N 2^{3i/2} i^2 K_n^2 L\right) = O(2^{3N/2} N^2 K_n^2 L). \quad (48)$$

It is noteworthy that although the complexity of the proposed algorithm seems to be exponential with respect to N , the actual complexity will not be excessively high since the value of N will not be very large in practice.

4) *Low-Complexity Bit Reallocation Algorithm:* The complexity of the above node selection algorithm is relatively high since Algorithm 1 is required to be executed multiple times. To reduce its computational complexity, we develop a bit reallocation idea and further propose a low-complexity algorithm in the following.

Specifically, we first initialize the selected node set as $\Omega = \{1, 2, \dots, N\}$ and execute the proposed MCSCA algorithm once to obtain the optimized quantization bit numbers $\{\bar{X}_{nj}\}$ (before rounding down). Then, a discrete solution can be obtained by performing the floor operation on each \bar{X}_{nj} , i.e., $X_{nj} = \lfloor \bar{X}_{nj} \rfloor$, $n \in \Omega$, $j \in [1, 2K_n]$. Next, we propose to iteratively increase the quantization bit number $X_{n'j'}$ by one bit, where n' and j' is obtained by $[n', j'] = \arg \min_{n,j} \text{CRLB}_{\hat{\theta}}|_{X_{nj}=X_{nj}+1}$. In other words, we choose the most important signal sample among all the receivers, i.e., increase the quantization bit number of this signal sample can

Algorithm 3 Proposed Low-Complexity Bit Reallocation Algorithm**Input:** $\{\hat{\tau}_n\}$, $\{\hat{\alpha}_n\}$, $\{\sigma_n^2\}$, $\{B_n\}$, $\{P_n\}$, $\{g_n\}$ and N_0 .**Output:** $\{X_{nj}^*\}$, W^* and Ω^* .

- 1: **Initialize** $\text{CRLB}_{opt} = +\infty$ and $\Omega^* = \{1, 2, \dots, N\}$.
- 2: Execute Algorithm 1 based on Ω^* to obtain $\{\bar{X}_{nj}\}$;
- 3: Set $X_{nj} = \lfloor \bar{X}_{nj} \rfloor$, $n \in \Omega$, $j \in [1, 2K_n]$;
- 4: **while** $\text{CRLB}_{opt} > \epsilon$ **do**
- 5: **for** $n = 1 : N$ **do**
- 6: **for** $j = 1 : 2K_n$ **do**
- 7: $X_{nj} = X_{nj} + 1$;
- 8: Calculate $\text{CRLB}_{\hat{\theta}}$ according to (21);
- 9: **if** $\text{CRLB}_{\hat{\theta}} \leq \text{CRLB}_{opt}$ **then**
- 10: $\text{CRLB}_{opt} = \text{CRLB}_{\hat{\theta}}$;
- 11: $n' = n$, $j' = j$;
- 12: **end if**
- 13: $X_{nj} = X_{nj} - 1$;
- 14: **end for**
- 15: **end for**
- 16: $X_{n'j'} = X_{n'j'} + 1$;
- 17: **end while**
- 18: Set $X_{nj}^* = X_{nj}$;
- 19: **for** $n = 1 : N$ **do**
- 20: **if** $\sum_j X_{nj} = 0$ **then**
- 21: $\Omega^* = \Omega^* \setminus n$;
- 22: **end if**
- 23: **end for**
- 24: Set W^* to be the minimum integer that satisfies (23);

reduce the CRLB most significantly. Repeat this process until the resulting CRLB satisfies the constraint (24b). The final channel use number W^* is set to be the minimum integer that satisfies the MAC capacity constraint (23). The details are presented in Algorithm 3.

In terms of computational complexity, we can see the complexity orders of Algorithms 2 and 3 are the same. However, it is straightforward to see that the actual complexity of Algorithm 3 is much lower than that of Algorithm 2, since the proposed MCSCA algorithm only needs to be run once in Algorithm 3.

V. SIMULATION RESULTS

In this section, we provide numerical results to evaluate the performance of the proposed HISDCS scheme and draw useful insights. Without loss of generality, we consider a common linear topology of the sensing receivers, as illustrated in Fig. 1. Unless otherwise specified, $N = 5$ sensing receivers are considered, and they are located equidistantly in a straight line with 50 m spacing. The transmitter is located 1000 m away from this line. We assume that the target is located between the transmitter and receivers, uniformly distributed in the $100 \text{ m} \times 50 \text{ m}$ region 50 m away from the line of sensing receivers. In our simulations, the sensing signal is set to be a Gaussian pulse signal, i.e., $s(t) = \frac{2^{0.25}}{T^{0.5}} e^{-\frac{\pi t^2}{T^2}}$ with $T = 2 \times 10^{-8}$ s. The carrier frequency, bandwidth and Nyquist sampling period are $f_c = 3.55$ GHz, $B = 50$ MHz and $T_s = \frac{1}{2B} = 10^{-8}$

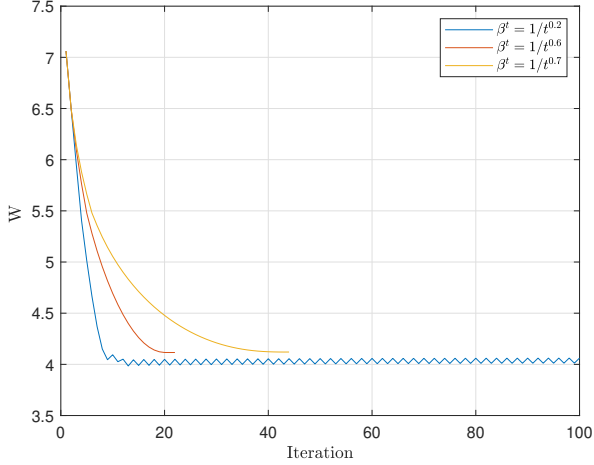


Fig. 3. Convergence behavior of the proposed MCSCA algorithm

s, respectively. Considering that the main lobe of $s(t)$ is in $-1.5T \leq t \leq 1.5T$, the sampling duration is set to $T_d = 4T = 8 \times 10^{-8}$ s, which is relatively large to contain the main lobe of $s(t)$. Therefore, the number of sampling points within one pulse for the proposed scheme is $K_n = \frac{T_d}{T_s} + 2 = 10$. Besides, the line-of-sight (LOS) model is employed to model the channels from the transmitter to the target, from the target to the receivers, and from the receivers to the FC, which is given by² [38]

$$L = 32.4 + 20 \log_{10}(d(\text{km})) + 20 \log_{10}(f_c(\text{GHz}))(\text{dB}), \quad (49)$$

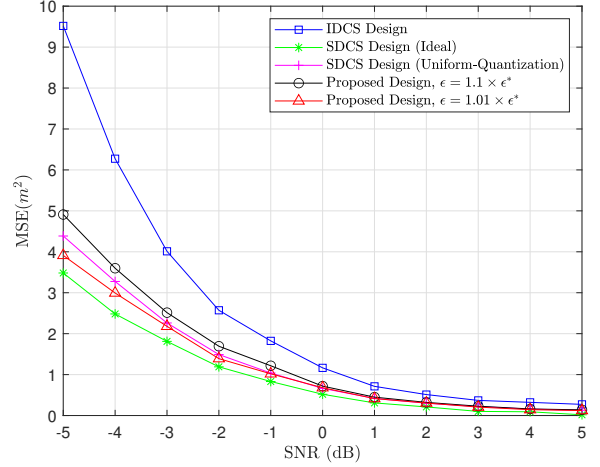
where L is the squared pathloss coefficient in dB, d is the distance between nodes.

For comparison, the following three baselines are considered: 1) A TOA based IDCS scheme, where each receiver only sends the estimated time delay $\hat{\tau}_n$ and effective reflecting coefficient $\hat{\alpha}_n$ to the FC for target localization based on the ML rule; 2) A uniform-quantization SDCS scheme, where each echo signal sample is uniformly quantized using 8 bits and then transmitted to the FC for localization; 3) An ideal SDCS scheme with unlimited communication capacity, i.e., assuming perfect echo signals are available at the FC.

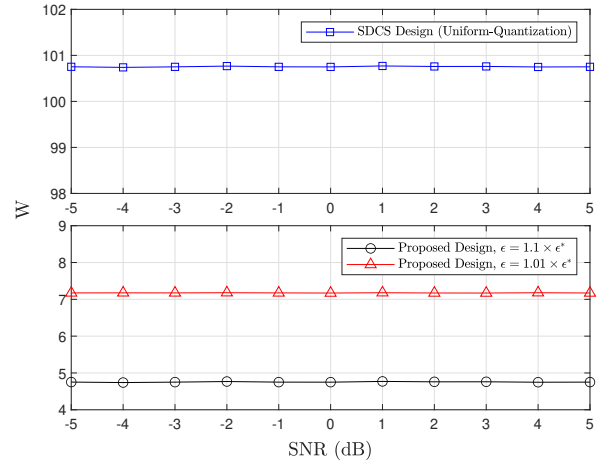
First, Fig. 3 plots the convergence behavior of the MCSCA algorithm under different choices of the step size β^t . It is shown that by choosing a feasible initial point and a proper step size, the proposed MCSCA algorithm is able to converge within 20 iterations. Besides, we can see that choosing a proper step size is very important for the proposed algorithm, since a small step size can result in a slow convergence rate, while selecting a large step size may induce oscillations.

Then, we compare in Fig. 4 the MSE performance and the average channel use number W between the baseline designs and the proposed HISDCS design under different SNR

²The sensing signal transmitted might propagate through a primary LOS path along with some NLOS paths before reaching the receiver. Normally, only the LOS path is exploited for localization, while the NLOS paths can be treated as a part of the clutter.



(a) MSE performance comparison under different SNR regimes



(b) Channel use number comparison under different SNR regimes

Fig. 4. Comparison between the proposed and baseline designs under different SNR regimes

regimes. It can be observed that in the medium-to-low SNR regime, the proposed HISDCS scheme outperforms the IDCS design in terms of MSE performance. Besides, it is worth noting that employing a smaller ϵ in constraint (24b) enhances the MSE performance of the HISDCS design. Especially when ϵ is set to $1.01 \times \epsilon^*$ (ϵ^* denotes the minimum achievable CRLB as mentioned in Section IV), the proposed HISDCS scheme outperforms the uniform-quantization SDCS scheme and its performance is remarkably close to the ideal SDCS design, which is regarded as the localization performance lower bound. Besides, from Fig. 4 (b), it is evident that the proposed HISDCS scheme significantly reduces the communication overhead as compared to the uniform-quantization SDCS scheme, since the former only needs 8 channel uses, while almost 101 channel uses are required by the latter.

Fig. 5 presents the MSE performance and average channel use number comparison between the baseline designs and the proposed HISDCS design under different numbers of sensing receivers N , where we set the average SNR to 0 dB. From

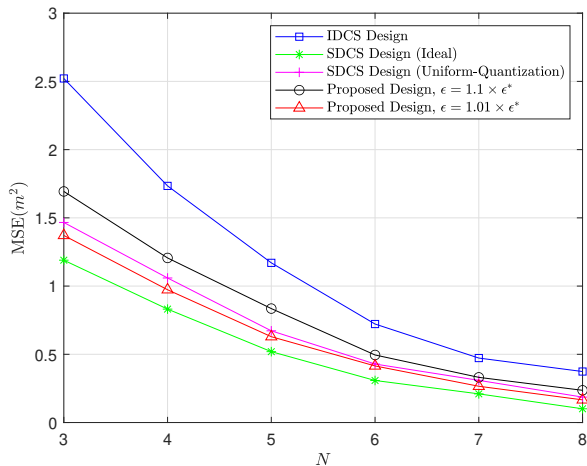
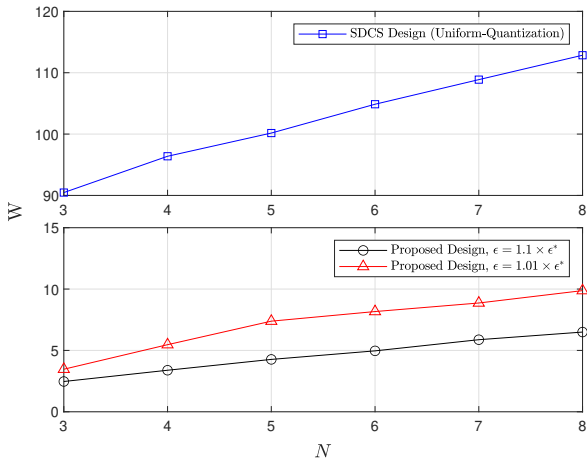
(a) MSE performance comparison under different N (b) Channel use number comparison under different N

Fig. 5. Comparison between the proposed and baseline designs under different numbers of sensing receivers

Fig. 5 (a), it is seen that the localization performance of the proposed HISDCS scheme is superior to that of the IDCS scheme. Additionally, as N increases, the MSE of all the considered schemes decreases, which is reasonable since larger N implies higher cooperation gain which is beneficial for localization performance improvement. Besides, from Fig. 5 (b), it can be observed that the communication overhead of the proposed HISDCS scheme is substantially reduced as compared to that required by the uniform-quantization SDCS scheme, and with the increasing of N , there is a consistent decrease in W across all schemes, which is mainly due to the fact that the amount of information transmitted to the FC for localization performance improvement increases as N increases.

In Fig. 6, we show the average number of channel uses W required by the proposed HISDCS scheme with or without node selection, and compare the performance of the proposed node selection strategy with the low-complexity bit reallocation algorithm presented in Section IV. From this figure, it

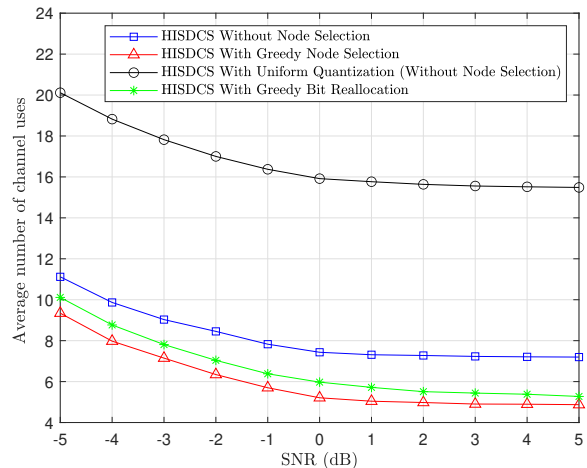


Fig. 6. Channel use number comparison under different SNR regimes

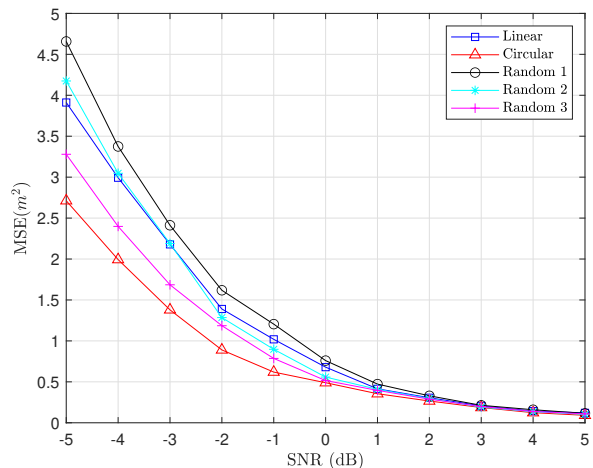


Fig. 7. MSE performance comparison under different topologies

is seen that compared to the scheme with the same number of quantization bits allocated to each receiver, the proposed MCSCA algorithm is much better in terms of communication cost. Besides, it can be observed that when node selection is employed, the number of channel uses W can be substantially reduced, for example, W can be reduced by 29.9% when $\text{SNR} = 0$ dB, indicating a reduction in communication overhead. Moreover, it is noteworthy that the proposed greedy bit reallocation algorithm requires a slightly higher average number of channel uses than the scheme with greedy node selection strategy, but it achieves a substantial reduction in computational complexity (as discussed in Section IV).

Next, we present in Fig. 7 the MSE performance of the proposed HISDCS scheme versus SNR, under different receiver topologies. In the circular topology case, the sensing receivers are symmetrically distributed on a 500 m radius circle around the transmitter and the target is uniformly distributed within the circle. We can observe from this figure that the localization performance under the circle topology is better than those under the linear topology and random topologies,

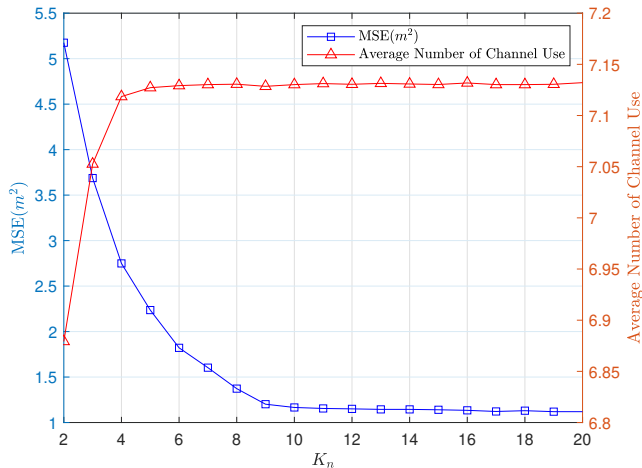


Fig. 8. MSE performance and required channel use number versus the number of sampling points K_n

which means that the receiver topology should be carefully designed in practice.

Then, we show in Fig. 8 the mean squared error (MSE) performance for target location estimation and the average channel use number W achieved by Algorithm 2 under different numbers of sampling points K_n . In this simulation, average signal-noise ratio (SNR) of the receivers is set to be -2 dB. From Fig. 4 (a), it can be seen that the localization performance improves with the increasing of K_n . However, when K_n is large, the localization performance improvement gradually saturates, and when K_n exceeds 14, the localization performance reaches a plateau. Besides, we can observe from Fig. 8 that the required number of channel uses W first increases as K_n increases, and then gradually stabilizes as K_n surpasses 4. Hence, the value of K_n needs to be carefully designed, for example, setting it to 10, which enables the achievement of favorable localization performance without incurring significant communication overhead, and the complexity of the MCSCA will not be excessively high.

Fig. 9 illustrates the impact of the sampling frequency f_s on the MSE performance and the average channel use number W , under the given sampling point number $K_n = 10$. It is observed that the best localization performance is achieved when f_s is about 100 MHz, otherwise, the performance gradually deteriorates. This is mainly due to the fact that, an excessively small or large f_s may result in the inability to extract useful localization information within the main lobe region of the echo signal under given K_n , consequently leading to a decline in the localization performance. Besides, we can see that the channel use number W barely changes as f_s varies, which is expected since K_n is fixed in this simulation.

Finally, we present in Fig. 10 the MSE performance and the average number of channel use W achieved by the proposed HISDCS scheme under different values of ϵ . It can be observed that as ϵ increases, the MSE gradually increases while W decreases. This is mainly owing to the fact that the demand for meeting the CRLB constraint gradually diminishes as ϵ increases, thus leading to localization performance degradation

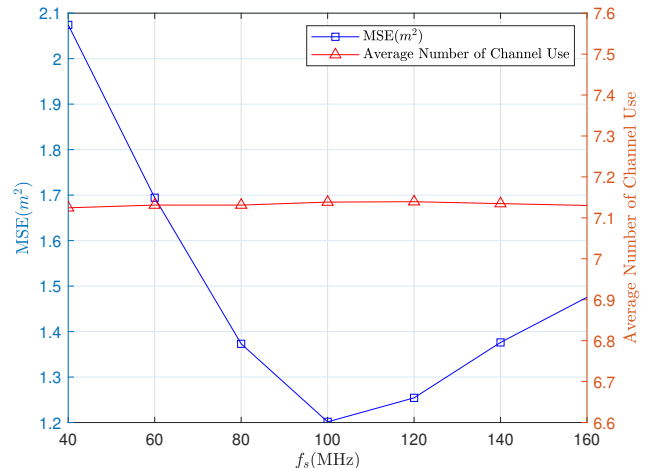


Fig. 9. MSE performance and required channel use number versus the sampling frequency f_s

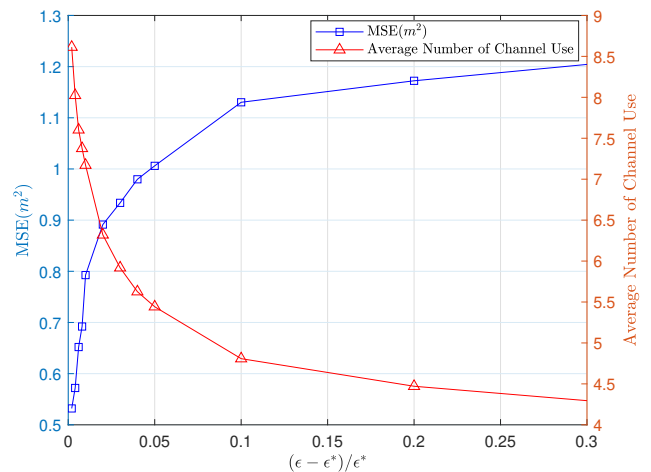


Fig. 10. MSE performance and the number of channel use comparison under different values of ϵ

and communication overhead reduction. Hence, there is a tradeoff between these two performance metrics that should be carefully considered based on the practical requirements.

VI. CONCLUSION

In this work, we investigated a cooperative sensing optimization problem in a multi-functional network. In order to improve the sensing accuracy while reduce the communication cost, we designed a HISDCS scheme, where each sensing receiver transmits the estimated time delay and effective reflecting coefficient, as well as the received sensing signal sampled around the estimated delay, to the FC. An optimization problem was formulated to minimize the number of channel uses under both CRLB and limited MAC capacity constraints. To tackle this problem, we proposed a MCSCA algorithm for quantization bit allocation and a greedy strategy for node selection. The convergence of the MCSCA algorithm to the set of KKT solutions was theoretically proved. Besides,

in order to further reduce the computational complexity, a greedy bit reallocation algorithm was proposed. Numerical simulations showed that our proposed HISDCS scheme is able to outperform the IDCS and SDCS schemes.

APPENDIX A PROOF OF LEMMA 1

According to [39], if we can prove that when $t \rightarrow \infty$, the supremum and infimum of $\|\bar{\mathbf{x}}^t - \mathbf{x}^t\|$ are zeroes, then (40) must hold. The proof can be completed via the following two steps.

1. We first prove that $\liminf_{t \rightarrow \infty} \|\bar{\mathbf{x}}^t - \mathbf{x}^t\| = 0$.

Due to the strong convexity of $\bar{f}_0^t(\mathbf{x})$, we have

$$\begin{aligned} \nabla^T \bar{f}_0^t(\mathbf{x}^t) \mathbf{d}^t &\leq -\eta_1 \|\mathbf{d}^t\|^2 + \bar{f}_0^t(\bar{\mathbf{x}}^t) - \bar{f}_0^t(\mathbf{x}^t) \\ &\leq -\eta_1 \|\mathbf{d}^t\|^2, \end{aligned} \quad (50)$$

where $\eta_1 > 0$, $\mathbf{d}^t = \bar{\mathbf{x}}^t - \mathbf{x}^t$ and the last inequality is due to the fact $\bar{f}_0^t(\bar{\mathbf{x}}^t) - \bar{f}_0^t(\mathbf{x}^t) \leq 0$ always holds since $\bar{\mathbf{x}}^t$ is the optimal solution of the problem (39), whereas \mathbf{x}^t is a feasible solution. Besides, since the gradient of $f_0(\mathbf{x})$ is Lipschitz continuous, we can obtain

$$\begin{aligned} f_0(\mathbf{x}^{t+1}) &\stackrel{(a)}{\leq} f_0(\mathbf{x}^t) + \eta_2 \beta^t \nabla^T f_0(\mathbf{x}^t) \mathbf{d}^t \\ &\quad + L_0 (\eta_2)^2 (\beta^t)^2 \|\mathbf{d}^t\|^2 \\ &\stackrel{(b)}{\leq} f_0(\mathbf{x}^t) - \eta_1 \eta_2 \beta^t \|\mathbf{d}^t\|^2 + O(\beta^t), \end{aligned} \quad (51)$$

where $L_0 > 0$, (a) is due to $\mathbf{x}^{t+1} = \mathbf{x}^t + \eta_2 \beta^t \mathbf{d}^t$, $\eta_2 > 0$ ((38) is a convex problem) and the Lipschitz gradient continuity of $f_0(\mathbf{x})$, and in (b), we use (50) and the fact that $\|\nabla^T \bar{f}_0(\mathbf{x}^t) - \nabla^T f_0(\mathbf{x}^t)\| = 0$.

Then, we prove $\liminf_{t \rightarrow \infty} \|\bar{\mathbf{x}}^t - \mathbf{x}^t\| = 0$ by contradiction. Assuming that there exists a positive constant ρ such that positive $\liminf_{t \rightarrow \infty} \|\bar{\mathbf{x}}^t - \mathbf{x}^t\| \geq \rho > 0$ holds, then we can easily find a sequence of \mathbf{d}^t that satisfies $\|\mathbf{d}^t\| \geq \rho$ for all t . Thus by choosing a sufficiently large t_0 , there always exists $\bar{\eta} > 0$ such that

$$f_0(\mathbf{x}^{t+1}) - f_0(\mathbf{x}^t) \leq -\beta^t \bar{\eta} \|\mathbf{d}^t\|^2, \forall t \geq t_0, \quad (52)$$

therefore, it follows from (52) that

$$f_0(\mathbf{x}^t) - f_0(\mathbf{x}^{t_0}) \leq -\bar{\eta} (\rho)^2 \sum_{j=t_0}^t \beta^j. \quad (53)$$

By letting $t \rightarrow \infty$, (53) contradicts the boundedness of $\{f_0(\mathbf{x}^t)\}$ given the fact that $\sum_{j=t_0}^{\infty} \beta^j = \infty$. Therefore, we have $\liminf_{t \rightarrow \infty} \|\bar{\mathbf{x}}^t - \mathbf{x}^t\| = 0$.

2. Then, we prove $\limsup_{t \rightarrow \infty} \|\bar{\mathbf{x}}^t - \mathbf{x}^t\| = 0$.

It follows from the Lipschitz continuity and strong convexity of $\bar{f}_i^t(\mathbf{x})$, $i = 0, \dots, m$ that [36]

$$\|\bar{\mathbf{x}}^{t_1} - \bar{\mathbf{x}}^{t_2}\| \leq \hat{L} \|\mathbf{x}^{t_1} - \mathbf{x}^{t_2}\| + e(t_1, t_2), \quad (54)$$

where $\hat{L} > 0$ and $\lim_{t_1, t_2 \rightarrow \infty} e(t_1, t_2) = 0$. Then, similar to the previous step, we prove $\limsup_{t \rightarrow \infty} \|\bar{\mathbf{x}}^t - \mathbf{x}^t\| = 0$ by contradiction.

Suppose that $\limsup_{t \rightarrow \infty} \|\bar{\mathbf{x}}^t - \mathbf{x}^t\| > 0$, since we have proved $\liminf_{t \rightarrow \infty} \|\bar{\mathbf{x}}^t - \mathbf{x}^t\| = 0$, it follows that there exists

a $\delta > 0$ such that both $\|\mathbf{d}^t\| \geq 2\delta$ and $\|\mathbf{d}^t\| < \delta$ holds for infinitely many t . Thus, we can always find an infinite set of indexes, denoted by \mathcal{T} , which satisfies the following property: for any $\forall t \in \mathcal{T}$, there exists $t_2 > t$, such that

$$\begin{aligned} \|\mathbf{d}^t\| &\leq \delta, \\ \|\mathbf{d}^{t_2}\| &\geq 2\delta, \\ \delta &< \|\mathbf{d}^n\| < 2\delta, t < n < t_2, \end{aligned} \quad (55)$$

holds. Then, based on (55), we have

$$\begin{aligned} \delta &\leq \|\mathbf{d}^{t_2}\| - \|\mathbf{d}^t\| \\ &\leq \|\mathbf{d}^{t_2} - \mathbf{d}^t\| \\ &= \|(\bar{\mathbf{x}}^{t_2} - \bar{\mathbf{x}}^t) - (\mathbf{x}^{t_2} - \mathbf{x}^t)\| \\ &\leq \|\bar{\mathbf{x}}^{t_2} - \bar{\mathbf{x}}^t\| + \|\mathbf{x}^{t_2} - \mathbf{x}^t\| \\ &\stackrel{(a)}{\leq} (1 + \hat{L}) \|\mathbf{x}^{t_2} - \mathbf{x}^t\| + e(t_2, t) \\ &= (1 + \hat{L}) \|\mathbf{x}^{t_2} - \mathbf{x}^{t_2-1} + \mathbf{x}^{t_2-1} - \mathbf{x}^{t_2-2} + \dots \\ &\quad + \mathbf{x}^{t+1} - \mathbf{x}^t\| + e(t_2, t) \\ &\leq (1 + \hat{L}) \sum_{n=t}^{t_2-1} \hat{\eta} \beta^n \|\mathbf{d}^n\| + e(t_2, t) \\ &\leq 2\delta \hat{\eta} (1 + \hat{L}) \sum_{n=t}^{t_2-1} \beta^n + e(t_2, t), \end{aligned} \quad (56)$$

where $\hat{\eta} > 0$ and (a) is obtained by resorting to (54). Then we obtain

$$\liminf_{t \rightarrow \infty} \sum_{n=t}^{t_2-1} \beta^n \geq \delta_1 = \frac{1}{2\hat{\eta}(1 + \hat{L})} > 0. \quad (57)$$

Invoking (52), there exists $\bar{\eta} > 0$, for $\forall t \in \mathcal{T}$, such that

$$f_0(\mathbf{x}^{n+1}) - f_0(\mathbf{x}^n) \leq -\beta^n \bar{\eta} \|\mathbf{d}^n\|^2, t < n < t_2, \quad (58)$$

then for sufficiently large t we have

$$f_0(\mathbf{x}^{t_2}) - f_0(\mathbf{x}^t) \leq -\bar{\eta} \delta^2 \sum_{n=t}^{t_2-1} \beta^n. \quad (59)$$

Since the convergence of $\{f_0(\mathbf{x}^t)\}$, there must be $\liminf_{t \rightarrow \infty} \sum_{n=t}^{t_2-1} \beta^n = 0$ which contradicts (57). Therefore, it can be shown that $\limsup_{t \rightarrow \infty} \|\bar{\mathbf{x}}^t - \mathbf{x}^t\| = 0$.

Combining the results of the above two steps, we have $\lim_{t \rightarrow \infty} \|\bar{\mathbf{x}}^t - \mathbf{x}^t\| = 0$, which completes the proof.

REFERENCES

- [1] M. Chen, M.-M. Zhao, A. Liu, M. Li, and M. Lei, "Cooperative sensing optimization over multiple access channel with limited backhaul capacity," in *2024 IEEE 35th Annual International Symposium on Personal, Indoor and Mobile Radio Communications (PIMRC)*, accepted for publication, 2024.
- [2] Y. Cui, F. Liu, X. Jing, and J. Mu, "Integrating sensing and communications for ubiquitous IoT: Applications, trends, and challenges," *IEEE Netw.*, vol. 35, no. 5, pp. 158–167, 2021.
- [3] F. Liu, C. Masouros, A. P. Petropulu, H. Griffiths, and L. Hanzo, "Joint radar and communication design: Applications, state-of-the-art, and the road ahead," *IEEE Trans. Commun.*, vol. 68, no. 6, pp. 3834–3862, 2020.
- [4] J. A. Zhang, M. L. Rahman, K. Wu, X. Huang, Y. J. Guo, S. Chen, and J. Yuan, "Enabling joint communication and radar sensing in mobile networks—a survey," *IEEE Commun. Surv. Tutor.*, vol. 24, no. 1, pp. 306–345, 2021.

- [5] A. Liu, Z. Huang, M. Li, Y. Wan, W. Li, T. X. Han, C. Liu, R. Du, D. K. P. Tan, J. Lu *et al.*, "A survey on fundamental limits of integrated sensing and communication," *IEEE Commun. Surv. Tutor.*, vol. 24, no. 2, pp. 994–1034, 2022.
- [6] F. Liu, Y. Cui, C. Masouros, J. Xu, T. X. Han, Y. C. Eldar, and S. Buzzi, "Integrated sensing and communications: Toward dual-functional wireless networks for 6G and beyond," *IEEE J. Sel. Areas Commun.*, vol. 40, no. 6, pp. 1728–1767, 2022.
- [7] N. Patwari, J. N. Ash, S. Kyperountas, A. O. Hero, R. L. Moses, and N. S. Correal, "Locating the nodes: cooperative localization in wireless sensor networks," *IEEE Signal Process. Mag.*, vol. 22, no. 4, pp. 54–69, 2005.
- [8] W. Meng, L. Xie, and W. Xiao, "Optimality analysis of sensor-source geometries in heterogeneous sensor networks," *IEEE Trans. Wirel. Commun.*, vol. 12, no. 4, pp. 1958–1967, 2013.
- [9] Y. Zhu, S. Xing, Y. Zhang, F. Yan, and L. Shen, "Localisation algorithm with node selection under power constraint in software-defined sensor networks," *IET Communications*, vol. 11, no. 13, pp. 2035–2041, 2017.
- [10] A. H. Sayed, A. Tarighat, and N. Khajehnouri, "Network-based wireless location: challenges faced in developing techniques for accurate wireless location information," *IEEE Signal Process. Mag.*, vol. 22, no. 4, pp. 24–40, 2005.
- [11] Y. Xiong, N. Wu, H. Wang, and J. Kuang, "Cooperative detection-assisted localization in wireless networks in the presence of ranging outliers," *IEEE Trans. Commun.*, vol. 65, no. 12, pp. 5165–5179, 2017.
- [12] J. M. Pak, C. K. Ahn, P. Shi, Y. S. Shmaliy, and M. T. Lim, "Distributed hybrid particle/fir filtering for mitigating NLOS effects in toa-based localization using wireless sensor networks," *IEEE Trans. Ind. Electron.*, vol. 64, no. 6, pp. 5182–5191, 2016.
- [13] N. Wu, Y. Xiong, H. Wang, and J. Kuang, "A performance limit of TOA-based location-aware wireless networks with ranging outliers," *IEEE Commun. Lett.*, vol. 19, no. 8, pp. 1414–1417, 2015.
- [14] H.-J. Shao, X.-P. Zhang, and Z. Wang, "Efficient closed-form algorithms for AOA based self-localization of sensor nodes using auxiliary variables," *IEEE Trans. Signal Process.*, vol. 62, no. 10, pp. 2580–2594, 2014.
- [15] G. Wang and H. Chen, "An importance sampling method for TDOA-based source localization," *IEEE Trans. Wirel. Commun.*, vol. 10, no. 5, pp. 1560–1568, 2011.
- [16] X. Li, "RSS-based location estimation with unknown pathloss model," *IEEE Trans. Wirel. Commun.*, vol. 5, no. 12, pp. 3626–3633, 2006.
- [17] C. Fan, L. Li, M.-M. Zhao, and M. Zhao, "An extended joint spatial and temporal cooperation model for the range-based localization problem," *IEEE Trans. Veh. Technol.*, vol. 68, no. 12, pp. 12121–12134, 2019.
- [18] M. Z. Win, A. Conti, S. Mazuelas, Y. Shen, W. M. Gifford, D. Dardari, and M. Chiani, "Network localization and navigation via cooperation," *IEEE Commun. Mag.*, vol. 49, no. 5, pp. 56–62, 2011.
- [19] S. Mazuelas, Y. Shen, and M. Z. Win, "Information coupling in cooperative localization," *IEEE Commun. Lett.*, vol. 15, no. 7, pp. 737–739, 2011.
- [20] N. Aghaie and M. A. Tinati, "Localization of wsn nodes based on NLOS identification using aoas statistical information," in *2016 24th Iranian Conference on Electrical Engineering (ICEE)*. IEEE, 2016, pp. 496–501.
- [21] Z. Wang, Q. He, and R. S. Blum, "Parameter estimation using quantized cloud MIMO radar measurements," in *2018 IEEE 10th Sensor Array and Multichannel Signal Processing Workshop (SAM)*, 2018, pp. 602–606.
- [22] S. Khalili, O. Simeone, and A. M. Haimovich, "Cloud radio-multistatic radar: Joint optimization of code vector and backhaul quantization," *IEEE Signal Process Lett.*, vol. 22, no. 4, pp. 494–498, 2014.
- [23] F. Xi, Y. Xiang, Z. Zhang, S. Chen, and A. Nehorai, "Joint angle and doppler frequency estimation for MIMO radar with one-bit sampling: A maximum likelihood-based method," *IEEE Trans. Aerosp. Electron. Syst.*, vol. 56, no. 6, pp. 4734–4748, 2020.
- [24] G. Zhang, W. Yi, P. K. Varshney, and L. Kong, "Direct target localization with quantized measurements in non-coherent distributed MIMO radar systems," *IEEE Trans. Geosci. Remote Sens.*, vol. 61, pp. 1–18, 2023.
- [25] S. Hadzic and J. Rodriguez, "Utility based node selection scheme for cooperative localization," in *2011 International Conference on Indoor Positioning and Indoor Navigation*. IEEE, 2011, pp. 1–6.
- [26] Z. Wang, Q. He, and R. S. Blum, "Target detection using quantized cloud MIMO radar measurements," *IEEE Trans. Signal Process.*, vol. 70, pp. 1–16, 2021.
- [27] V. K. Goyal, "Theoretical foundations of transform coding," *IEEE Signal Process. Mag.*, vol. 18, no. 5, pp. 9–21, 2001.
- [28] D. W. Bliss, "Cooperative radar and communications signaling: The estimation and information theory odd couple," in *2014 IEEE Radar Conference*, 2014, pp. 0050–0055.
- [29] W. R. Li, M. Li, A. Liu, and T. X. Han, "Design and optimization of cooperative sensing with limited backhaul capacity," in *IEEE 98th Vehicular Technology Conference (VTC)*, Hongkong, China, 2023.
- [30] S. M. Kay, *Fundamentals of statistical signal processing: estimation theory*. Prentice-Hall, Inc., 1993.
- [31] T. M. Cover, *Elements of information theory*. John Wiley & Sons, 1999.
- [32] S.-H. Park, O. Simeone, O. Sahin, and S. S. Shitz, "Fronthaul compression for cloud radio access networks: Signal processing advances inspired by network information theory," *IEEE Signal Process. Mag.*, vol. 31, no. 6, pp. 69–79, 2014.
- [33] D. Tse and P. Viswanath, *Fundamentals of wireless communication*. Cambridge university press, 2005.
- [34] M. Razaviyayn, "Successive convex approximation: Analysis and applications," Ph.D. dissertation, University of Minnesota, 2014.
- [35] D. A. Guimaraes, G. H. F. Floriano, and L. S. Chaves, "A tutorial on the CVX system for modeling and solving convex optimization problems," *IEEE Lat. Am. Trans.*, vol. 13, no. 5, pp. 1228–1257, 2015.
- [36] A. Liu, V. K. Lau, and B. Kananian, "Stochastic successive convex approximation for non-convex constrained stochastic optimization," *IEEE Trans. Signal Process.*, vol. 67, no. 16, pp. 4189–4203, 2019.
- [37] K.-Y. Wang, A. M.-C. So, T.-H. Chang, W.-K. Ma, and C.-Y. Chi, "Outage constrained robust transmit optimization for multiuser MISO downlinks: Tractable approximations by conic optimization," *IEEE Trans. Signal Process.*, vol. 62, no. 21, pp. 5690–5705, 2014.
- [38] T. S. Rappaport, Y. Xing, G. R. MacCartney, A. F. Molisch, E. Mellios, and J. Zhang, "Overview of millimeter wave communications for fifth-generation (5G) wireless networks—with a focus on propagation models," *IEEE Trans. Antennas Propag.*, vol. 65, no. 12, pp. 6213–6230, 2017.
- [39] W. Rudin *et al.*, *Principles of mathematical analysis*. McGraw-hill New York, 1964, vol. 3.